



OPEN

## High-precision and cost-efficient sequencing for real-time COVID-19 surveillance

Sung Yong Park<sup>1,3</sup>, Gina Faraci<sup>1,3</sup>, Pamela M. Ward<sup>2</sup>, Jane F. Emerson<sup>2</sup> & Ha Youn Lee<sup>1</sup>✉

COVID-19 global cases have climbed to more than 33 million, with over a million total deaths, as of September, 2020. Real-time massive SARS-CoV-2 whole genome sequencing is key to tracking chains of transmission and estimating the origin of disease outbreaks. Yet no methods have simultaneously achieved high precision, simple workflow, and low cost. We developed a high-precision, cost-efficient SARS-CoV-2 whole genome sequencing platform for COVID-19 genomic surveillance, CorvGenSurv (Coronavirus Genomic Surveillance). CorvGenSurv directly amplified viral RNA from COVID-19 patients' Nasopharyngeal/Oropharyngeal (NP/OP) swab specimens and sequenced the SARS-CoV-2 whole genome in three segments by long-read, high-throughput sequencing. Sequencing of the whole genome in three segments significantly reduced sequencing data waste, thereby preventing dropouts in genome coverage. We validated the precision of our pipeline by both control genomic RNA sequencing and Sanger sequencing. We produced near full-length whole genome sequences from individuals who were COVID-19 test positive during April to June 2020 in Los Angeles County, California, USA. These sequences were highly diverse in the G clade with nine novel amino acid mutations including NSP12-M755I and ORF8-V117F. With its readily adaptable design, CorvGenSurv grants wide access to genomic surveillance, permitting immediate public health response to sudden threats.

Pathogen whole genome sequencing informs evidence-based public health decisions by providing crucial data for disease transmission, new outbreak detection, and vaccine candidate selection<sup>1,2</sup>, as demonstrated by HIV<sup>3</sup>, tuberculous<sup>4</sup>, Ebola<sup>5,6</sup> and Zika<sup>7</sup> outbreaks. In the immediate response to COVID-19, several studies have demonstrated that genomic surveillance outcomes were not only comparable to epidemiological contact tracing data<sup>8–10</sup> but also capable of tracing previously unknown linked transmissions<sup>11</sup>. Genomic investigation informed the public health decisions to prevent further spread of SARS-CoV-2, including travel restrictions and stay-at-home orders in response to the identification of travel-related clusters and local clusters<sup>10</sup>. Rapid SARS-CoV-2 whole genome sequencing is therefore an essential public health measure.

SARS-CoV-2 whole genome sequencing also has important utility in the surveillance of amino acid mutations that may result in changes to viral protein physical structures<sup>12,13</sup>. Such changes in structure can potentially alter virus transmissibility<sup>14</sup>, disease severity<sup>15</sup>, or reduce vaccine efficacy<sup>16,17</sup>. Over 90 vaccines are currently in development<sup>18</sup> and spike protein based vaccine candidates have induced both neutralizing antibody and T-cell responses against SARS-CoV-2<sup>19</sup>. However, diverse mutations in viral proteins, as observed in GISAID<sup>20,21</sup> and Nextstrain<sup>22</sup>, may lower COVID-19 vaccine effectiveness<sup>16,17</sup>, as observed in influenza vaccines<sup>23,24</sup>. Similarly, mutations in therapeutic drug target regions such as RNA-dependent RNA polymerase (RdRP) can potentially lead to treatment failure<sup>25</sup>. Therefore, it is important to be able to surveil virus mutations in real-time to ensure the efficacy of prophylactic vaccines and therapeutic drugs.

The greatest barriers to the deployment of massive SARS-CoV-2 whole genome sequencing for routine use are the complexity and expense of the workflows. Current SARS-CoV-2 whole genome sequencing methods, including the widely-used ARTIC network protocol, generally rely on short-read amplifications and sequencing<sup>8,10–12,26–31</sup>. However, a high number of short-read amplifications increases the risk of genome coverage dropouts<sup>8</sup>. Minimizing this risk often requires deep sequencing coverage, resulting in high-sequencing cost. To date, no SARS-CoV-2 whole genome sequencing method has concurrently accomplished high-resolution, simple workflow, and low-cost.

<sup>1</sup>Department of Molecular Microbiology and Immunology, Keck School of Medicine, University of Southern California, Los Angeles, CA, USA. <sup>2</sup>Department of Clinical Pathology, Keck School of Medicine, University of Southern California, Los Angeles, CA, USA. <sup>3</sup>These authors contributed equally: Sung Yong Park and Gina Faraci. ✉email: hayoun@usc.edu

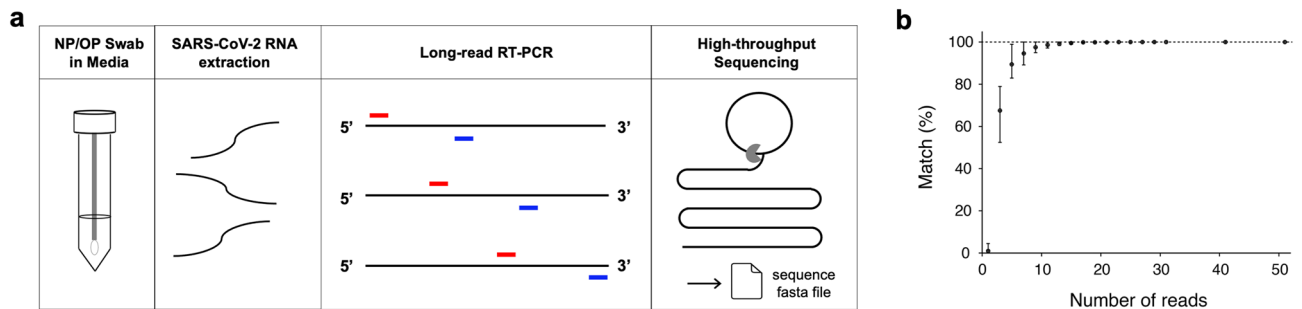


**Figure 1.** CorvGenSurv's workflow and precision. **(a)** Remnant NP/OP specimens from COVID-19 diagnostic testing were subject to SARS-CoV-2 RNA extraction. Viral RNA was amplified via three overlapping RT-PCRs (~ 10,000 base long each) and pooled SARS-CoV-2 amplicons of indexed COVID-19 specimens were then sequenced by long-read high-throughput single-molecule sequencing. The output fasta file was de-multiplexed and processed to produce the consensus sequence of each segment. Each COVID-19 specimen's three overlapping segments were assembled into a SARS-CoV-2 whole genome sequence. **(b)** CorvGenSurv's precision was tested by comparing the consensus sequence from a given number of reads with the USA-WA1/2020 control strain (GenBank: MN985325.1). When a consensus sequence was built from three reads, only 67% [52.4–78.9%] of the 1000 bootstrap runs' resulting consensus sequences were consistent with the correct sequence. When the number of the reads was greater or equal to 31, all 1000 bootstrap runs resulted in the correct sequence.

Herein, we introduce CorvGenSurv (Coronavirus Genomic Surveillance), an accurate and cost-efficient SARS-CoV-2 whole genome sequencing platform for COVID-19 genomic surveillance. We directly amplify viral RNA and sequence it in three segments using long-read, high-throughput sequencing. Sequencing of the SARS-CoV-2 whole genome in three segments prevents dropouts in genome coverage by minimizing ambiguous reads and eliminating assembly errors. CorvGenSurv is a streamlined, high-resolution, and cost-effective pipeline that facilitates the deployment of real-time SARS-CoV-2 whole genome sequencing for public health.

## Results

**Workflow of CorvGenSurv.** We extracted SARS-CoV-2 RNA from remnant COVID-19 positive NP/OP swab specimens in universal viral transport media. Rather than converting viral RNA to cDNA, we instead directly amplified viral RNA via long-read reverse transcriptase-polymerase chain reaction (RT-PCR). Three overlapping RT-PCR amplicons were produced for each specimen. Each specimen's three overlapping RT-PCR amplicons were then indexed, and multiplexed specimens sequenced by long-read high-throughput sequencing<sup>32,33</sup> (Fig. 1a). After de-multiplexing, we built the consensus sequence of each of the three segments, correcting sequencing errors. These overlapping consensus sequences were then assembled into a near full-length SARS-CoV-2 whole genome sequence for each COVID-19 case.

**Precision and accuracy of CorvGenSurv.** We measured the accuracy of CorvGenSurv by sequencing the genomic RNA of the USA-WA1/2020 control strain (GenBank: MN985325.1) provided by BEI Resources (NR-52285). The assembled near full-length SARS-CoV-2 sequence obtained by CorvGenSurv matched 100% to the sequence of this control strain. This accuracy was achieved by our error correction step during consensus sequence building. To assess how many reads are required to produce an accurate consensus sequence, we performed a bootstrap test, randomly sampling a given number of reads and building the consensus sequence of those reads. As shown in Fig. 1b, when three reads were sampled, only 67% [52.4–78.9%] of the 1000 bootstrap runs' resulting consensus sequences were consistent with the reference sequence of USA-WA1/2020. When we generated a consensus sequence from 31 or more reads, the consensus sequence of all 1000 bootstrap runs was identical to the control sequence. This 31-fold sequencing depth ensured the production of a SARS-CoV-2 whole genome sequence that perfectly matched the control sequence.

We also spot-checked the precision of CorvGenSurv by Sanger sequencing, the current gold standard for precision checking<sup>34</sup>. USA/CA-LAC-USC1 in Table 1 was selected, and a near full-length SARS-CoV-2 sequence was obtained by assembling a total of 49 overlapping segments that were sequenced by Sanger sequencing. The resulting Sanger sequence matched 100% to the corresponding USA/CA-LAC-USC1 sequence obtained by CorvGenSurv.

We observed two putative deletions in one sequence (USA/CA-LAC-USC2) that potentially originated from homopolymer sequencing errors. However, these errors were rare as we observed only two deletions out of 754,702 base calls ( $2.65 \times 10^{-6}$  per base). We have thus corrected these putative errors.

**COVID-19 specimen profiling.** We produced whole genome sequences of 25 Los Angeles County COVID-19 patients who tested positive at Keck Medicine of USC Clinical Laboratories by accessing their remnant NP/OP swab specimens. This study (HS-20-00326) was approved by the Institutional Review Board of the University of Southern California. Table 1 presented each specimen's collection date from April to June 2020 and COVID-19 test cycle threshold ( $C_t$ ) values.

Specimen ID	Collection date	C <sub>t</sub> -1	C <sub>t</sub> -2	Amino acid mutations	GISAID clade (Pango lineage)
USA/CA-LAC-USC1	4/13/20	18.58	18.72	NSP12-P323L, <b>NSP12-M755I</b> , S-D614G, N-R203K, N-G204R	GR (B.1.1)
USA/CA-LAC-USC2	4/13/20	24.84	25.44	NSP3-G1011X, <b>NSP3-F1659L</b> , NSP4-S312N, NSP12-P323L, S-D614G, N-R203K, N-G204R	GR (B.1.1)
USA/CA-LAC-USC3	4/14/20	24.18	24.96	NSP2-T85I, NSP12-P323L, NSP14-G44D, NSP16-S33R, S-D614G, S-D1184N, ORF3a-Q57H	GH (B.1)
USA/CA-LAC-USC4	5/5/20	20.06	20.46	NSP2-T85I, NSP12-P323L, S-D614G, ORF3a-Q57H	GH (B.1)
USA/CA-LAC-USC5	5/6/20	24.94	25.09	NSP3-G638S, NSP5-K90R, NSP6-Q208H, NSP12-P323L, NSP14-V287F, <b>ORF8-V117F</b> , S-F565L, S-D614G, N-R203K, N-G204R	GR (B.1.1.61)
USA/CA-LAC-USC6	5/9/20	28.25	28.48	NSP12-T85I, NSP12-P323L, NSP16-A188S, S-D614G, N-R203K, N-G204R	GR (B.1.1)
USA/CA-LAC-USC7	5/9/20	23.05	23.19	NSP3-D1214N, NSP12-P323L, S-D614G, N-R203K, N-G204R	GR (B.1.1)
USA/CA-LAC-USC8	5/18/20	17.34	17.10	NSP2-T85I, NSP12-P323L, S-D614G, S-P812L, ORF3a-Q57H, M-A68S, N-G34W	GH (B.1)
USA/CA-LAC-USC9	6/1/20	20.26	20.46	NSP2-K110N, NSP2-P191S, NSP12-P323L, S-D614G, ORF7a-H73R, N-S194L	G (B.1.397)
USA/CA-LAC-USC10	6/2/20	23.34	23.69	NSP2-K110N, NSP2-P191S, NSP12-P323L, S-D614G, N-S194L	G (B.1.397)
USA/CA-LAC-USC11	6/4/20	19.21	19.04	NSP12-P323L, S-D614G, ORF8-I47F, N-R203K, N-G204R	GR (B.1.1.172)
USA/CA-LAC-USC12	6/5/20	16.79	16.42	NSP3-Q203H, NSP12-P323L, NSP15-E223G, S-D614G, <b>N-P122H</b> , N-R203K, N-G204R	GR (B.1.1.228)
USA/CA-LAC-USC13	6/6/20	23.60	24.01	NSP2-T85I, NSP2-A361V, NSP8-L35F, NSP12-P323L, NSP13-K460R, NSP16-M17I, S-D614G, S-K1191N, ORF3a-Q57H, ORF3a-T175I	GH (B.1.166)
USA/CA-LAC-USC14	6/8/20	15.61	15.51	<b>NSP3-P192H</b> , NSP3-T1288I, NSP12-P323L, NSP13-P238S, S-D614G, N-Q9H, N-S194L	G (B.1)
USA/CA-LAC-USC15	6/9/20	18.59	18.64	<b>NSP3-I1672S</b> , NSP8-S177L, NSP12-P323L, S-D614G, S-P807R	G (B.1)
USA/CA-LAC-USC16	6/9/20	26.52	27.18	NSP12-P323L, S-T286I, S-A522V, S-D614G, ORF3a-Q57H	GH (B.1.110)
USA/CA-LAC-USC17	6/9/20	29.39	30.39	NSP1-V116M, NSP2-T85I, NSP3-A231V, NSP5-L89F, NSP12-P323L, NSP16-V294F, S-D614G, ORF3a-Q57H, ORF8-S24L	GH (B.1.595)
USA/CA-LAC-USC18	6/9/20	17.07	16.83	NSP2-K110N, NSP2-P191S, NSP12-P323L, NSP16-P236S, S-Y144X, S-D614G, N-S194L	G (B.1.397)
USA/CA-LAC-USC19	6/10/20	26.27	26.37	NSP12-P323L, S-D614G, ORF7a-P34S, N-R203K, N-G204R	GR (B.1.1)
USA/CA-LAC-USC20	6/10/20	27.65	28.42	NSP12-P323L, S-G142C, S-R214C, S-D614G, ORF3a-P159S, N-R203K, N-G204R, N-Q229H	GR (B.1.1.132)
USA/CA-LAC-USC21	6/11/20	24.27	24.82	NSP2-T85I, NSP3-P108L, NSP12-P323L, S-R21I, S-Y28H, S-D614G, ORF3a-Q57H, ORF8-S24L, N-G34W	GH (B.1.336)
USA/CA-LAC-USC22	6/11/20	24.48	25.19	NSP2-T85I, <b>NSP3-S702F</b> , NSP3-T1830I, <b>NSP4-Q77H</b> , NSP12-P323L, S-D614G, ORF3a-Q57H	GH (B.1)
USA/CA-LAC-USC23	6/22/20	29.29	29.45	NSP2-T85I, NSP12-T293I, NSP12-P323L, S-V308L, S-D614G, ORF3a-Q57H, N-S183Y	GH (B.1.369)
USA/CA-LAC-USC24	6/22/20	28.15	28.19	NSP12-P323L, NSP16-D102Y, S-D614G, N-S194L	G (B.1.558)
USA/CA-LAC-USC25	6/22/20	28.59	28.63	NSP2-A360V, <b>NSP3-D1148N</b> , NSP6-L37F, NSP12-P323L, N-R203K, N-G204R, S-L5F, S-D614G	GR (B.1.1)

**Table 1.** Amino acid mutations, clade and lineage of 25 whole genome sequences from COVID-19 remnant NP/OP specimens. Novel amino acid mutations that were not observed among 28,176 global SARS-CoV-2 sequences in GISAID are in bold. C<sub>t</sub>-1 targeted the ORF1/a-b non-structural region and C<sub>t</sub>-2 a conserved region in the structural protein envelope E-gene. qRT-PCR was performed using the Roche COBAS system.

Figure 2a presented the maximum likelihood tree of these 25 Los Angeles sequences along with 1,215 sequences from the state of California archived in GISAID<sup>20,21</sup> as of July 27th, 2020. The most recent common ancestor sequence of the 25 strains (grey circle in Fig. 2a) had three nucleotide substitutions from the reference sequence, Wuhan-Hu-1, and two amino acid changes, P323L in the RNA-dependent RNA polymerase (RdRP, NSP12) and D614G in the S protein<sup>12,35</sup>. As expected, sequences of specimens collected from April to May (purple numbers in Fig. 2a) were located closer to the root of tree than those of specimens collected in June (blue numbers in Fig. 2a). Ten of the 25 sequences shared additional mutations of R203K and G204R in the N (nucleocapsid) protein (skyblue circle in Fig. 2a) as part of the GR-clade<sup>20,21</sup>. Eight other sequences had mutations of T85I in the NSP2 protein and Q57H in the ORF3a protein (red circle in Fig. 2a) as part of the GH-clade<sup>20,21</sup>. Five other sequences shared the mutation S194L in the N protein (purple circle in Fig. 2a) as part of the G-clade<sup>20,21</sup>. One sequence (USA/CA-LAC-USC15) had a unique mutation lineage amongst the sampled 25 sequences as part of the G-clade<sup>20,21</sup> (Fig. 2a). Another sequence (USA/CA-LAC-USC16) had a unique mutation lineage as part of the GH clade<sup>20,21</sup>. These 25 sequences reflect the high viral diversity observed in California within the G, GR, and GH clades<sup>35,36</sup>.

Figure 2b marked the amino acid changes of each of our 25 sequences in reference to the Wuhan-Hu-1 sequence. We reported a total of nine new amino acid mutations that were not observed among 28,176 global SARS-CoV-2 sequences in GISAID<sup>20,21</sup>. These include M755I in RdRP (NSP12) and V117F in the ORF8 protein (Table 1).

We compared the prevalence of each amino acid mutation from Wuhan-Hu-1 that had greater than 2% frequency either globally, in the USA, or in California as of July, 2020 (Fig. 2c). Mass circulation of G clade strains

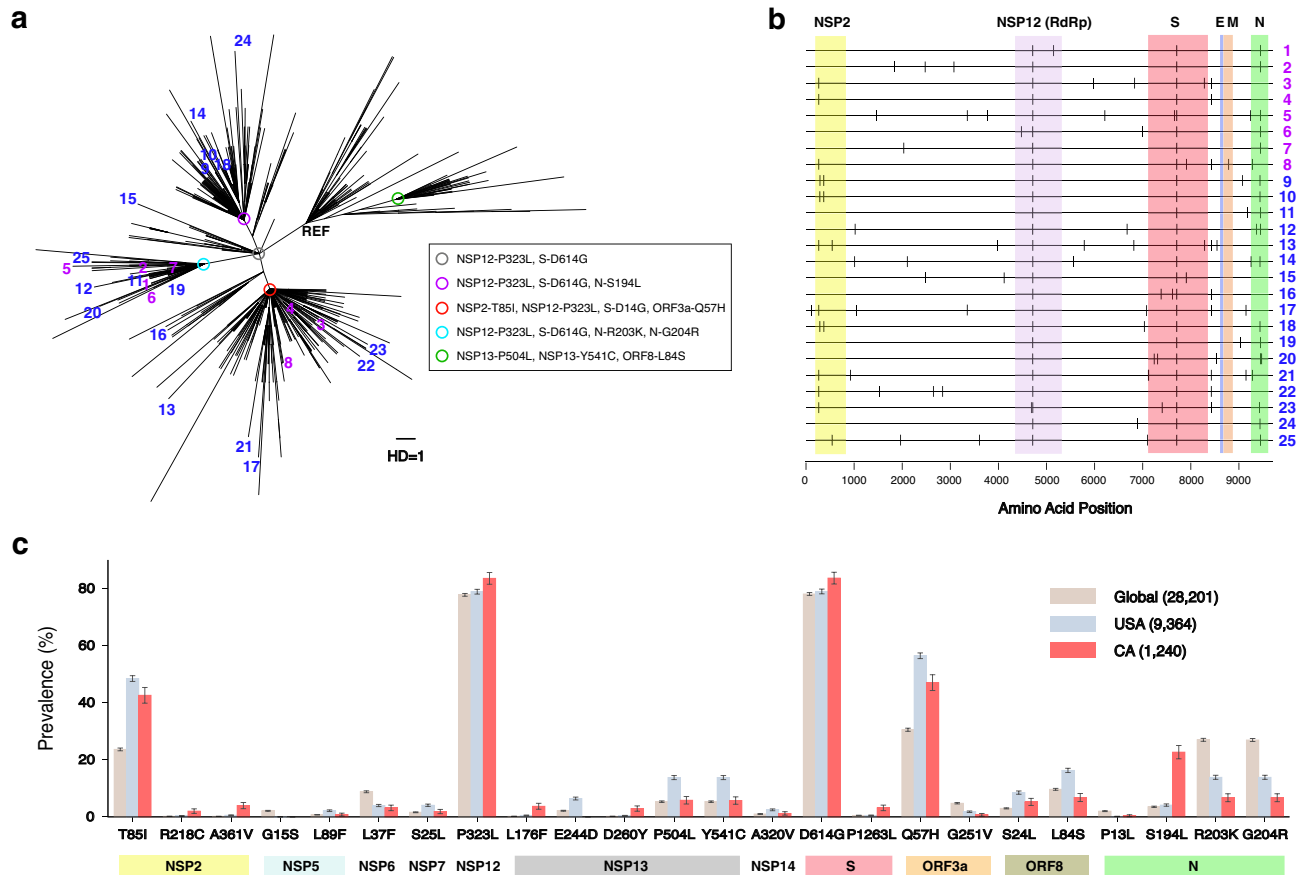


**Figure 2.** Maximum likelihood tree analysis and amino acid mutations of 25 SARS-CoV-2 whole genome sequences obtained by CorvGenSurv. **(a)** Maximum likelihood tree of 25 SARS-CoV-2 sequences obtained by CorvGenSurv along with sequences collected in California, USA. A total of 1215 SARS-CoV-2 sequences collected from California, USA were downloaded from GISAID<sup>20,21</sup> as of July 27th, 2020. Our sequences were obtained from 25 remnant specimens from COVID-19 testing between April 13th and June 22nd, 2020 from Los Angeles County, California, USA. Specimens collected from April to May 2020 were colored purple and those collected in June were colored blue. Sequences of specimens USA/CA-LAC-USC1 to USA-CA-LAC-USC25 in Table 1 were denoted by 1 to 25 in this tree. All 25 sequences were classified as G clade with mutations P323L in NSP12 (RdRp) and D614G in S protein (grey circle). Different ancestral sequences were presented by circles in different colors with common mutations of each lineage presented in the box. The unit branch length (one nucleotide base substitution) was denoted as “HD=1”. **(b)** Each of our 25 sequences’ amino acid mutations from Wuhan-Hu-1 (MN908947) were marked using Highlighter ([https://www.hiv.lanl.gov/content/sequence/HIGHLIGHT/highlighter\\_top.html](https://www.hiv.lanl.gov/content/sequence/HIGHLIGHT/highlighter_top.html)). The regions of NSP2, NSP12 (RdRp), S, E, M, and N were presented by colored boxes. **(c)** The prevalence of each amino acid mutation with greater than 2% frequency either globally, in the USA, or in California. A total of 28,176 global sequences were downloaded from GISAID<sup>20,21</sup>.

were confirmed by around 80% prevalence of P323L in RdRp and D614G in the S protein globally. In USA and California, the prevalence of T85I in NSP2 and Q57H in ORF3a were observed to be above 40%, as shown in Fig. 2c. The prevalence of P1263L mutation in the S protein was sixfold greater in California than the global prevalence. Additionally, S194L mutation in the N protein was much more prevalent in California, compared to other regions.

**CorvGenSurv’s supply cost.** The development of a cost-effective SARS-CoV-2 genotyping protocol is crucial to expanding COVID-19 surveillance efforts. The per-specimen supply cost of our SARS-CoV-2 whole genome sequencing method was estimated to be \$33.8. This includes RNA extraction from NP/OP swab media (\$4.58), long-range RT-PCR (\$25.8), index PCR (\$2.6), and long-read high-throughput sequencing (\$0.82).

We estimated the per-specimen high-throughput sequencing cost by assessing the maximum number of specimens ( $N_m$ ) we can process in a single sequencing run. We observed that 31 or more reads would be required to produce an accurate consensus sequence (Fig. 1b). Therefore, we estimated how many reads are required on average to obtain a minimum of 31 reads per consensus sequence. The expected minimum value of  $N_g$  Poisson random variables is given by  $\sum_{k=1}^{\infty} [\gamma(k, \lambda) / \Gamma(k)]^{N_g}$ , where  $\lambda$  is the mean of the Poisson distribution,  $\gamma(k, \lambda)$  is the lower incomplete gamma function, and  $\Gamma(k)$  is the gamma function. Since we need three segments per specimen,  $N_g$  is given by  $3 \times N_m$ . We obtained around 1.58 million circular consensus sequence (CCS) reads

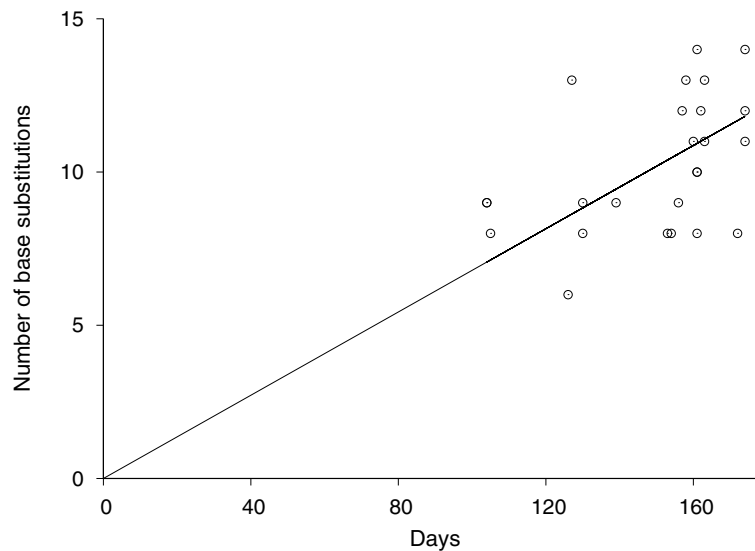


**Figure 3.** SARS-CoV-2 divergence. Our 25 Los Angeles sequences' number of base substitutions from the reference sequence Wuhan-Hu-1 (MN908947) was plotted against the collection time of each sequence as days from the reference sequence collection time, December 31st, 2019. The SARS-CoV-2 evolution rate was estimated to be  $8.62 \times 10^{-4}$  substitutions per site per year (95% confidence interval:  $7.96 \times 10^{-4}$  to  $9.24 \times 10^{-4}$ ) by linear regression (solid line).

with 99% accuracy for a library size of  $\sim 10$  kb from a single sequencing run. We estimated that 8779 specimens can be processed in a single sequencing run, where 60 reads per consensus sequence can be obtained on average to recover a minimum of 31 reads per consensus sequence. Similarly, if we aim to recover a minimum of 100 reads per consensus sequence as a conservative approach, around 3657 specimens can be processed in a single sequencing run. Assuming a sequencing cost of \$3000, this yields a per specimen sequencing cost of \$0.82 for large-scale sequencing efforts.

This estimated low-sequencing cost suggests a cost advantage over current short-read based SARS-CoV-2 whole genome sequencing methods<sup>8,10–12,26–30</sup>. The required time for CorvGenSurv is around 15 h for sample library preparation and 30 h for sequencing. Our cost-effective workflow may therefore enhance the implementation of real-time massive genomic SARS-CoV-2 surveillance.

**SARS-CoV-2 evolution rate.** We estimated the rate of SARS-CoV-2 evolution from the 25 genomes we obtained using a Bayesian phylogenetic reconstruction method<sup>37,38</sup>. The SARS-CoV-2 nucleotide evolution rate was estimated to be  $7.51 \times 10^{-4}$  substitutions per site per year [95% highest posterior density (HPD):  $2.04 \times 10^{-4}$  to  $1.34 \times 10^{-3}$ ]. The median divergence time was estimated to be December 5th, 2019 [95% HPD: December 16th, 2018–March 19th, 2020]. This estimate was 26 days prior to the first SARS-CoV-2 sequence Wuhan-Hu-1's sample collection time, December 31st, 2019.

The rate of SARS-CoV-2 evolution was also estimated by measuring the rate of divergence from the reference Wuhan-Hu-1 sequence. We plotted our sequences' number of nucleotide base differences from the Wuhan-Hu-1 sequence against sample collection time difference in Fig. 3. The nucleotide substitution rate in reference to Wuhan-Hu-1 was measured to be  $8.62 \times 10^{-4}$  substitutions per site per year (95% confidence interval:  $7.96 \times 10^{-4}$  to  $9.24 \times 10^{-4}$ ). This rate was consistent with the above Bayesian phylogenetic estimate.

**Influenza vaccination and evolution.** It has been reported that several SARS-CoV-2 variants of concern can potentially escape from vaccine-induced immunity<sup>16,17</sup>. The emergence and circulation of such variants has prompted efforts to continuously monitor SARS-CoV-2 evolution via real-time genomic surveillance<sup>39,40</sup>. To further demonstrate its importance, we analyzed influenza evolution in response to vaccination. Influenza has also been shown to escape from vaccine-induced immunity, as confirmed by serologic testing<sup>41</sup>. The WHO changed the 2019–2020 H1N1 Northern Hemisphere Flu vaccine strain from A/Michigan/45/2015 (grey diamond in Fig. 4a–c) to A/Brisbane/02/2018 (purple diamond in Fig. 4a–c)<sup>42</sup>. Our maximum likelihood tree analysis showed that influenza H1N1 Hemagglutinin (HA) sequences evolved away from this new vaccine strain. As shown in Fig. 4a, a total of 255 H1N1 Hemagglutinin (HA) sequences sampled in April 2019 were relatively close to the 2019–2020 H1N1 vaccine strain (purple diamond in Fig. 4a). However, we found that HA sequences collected in January 2020 (1140 sequences total) had evolved away from this vaccine strain. This rapid evolution was visualized in a two-dimensional map obtained by multidimensional scaling of the pairwise HA sequence distance matrix (Fig. 4b,c). As plotted in Fig. 4d, the nucleotide base difference from the vaccine sequence was significantly higher among the January 2020 sequences, compared to the April 2019 sequences (median distance 18 vs. 23,  $p < 0.001$ ).

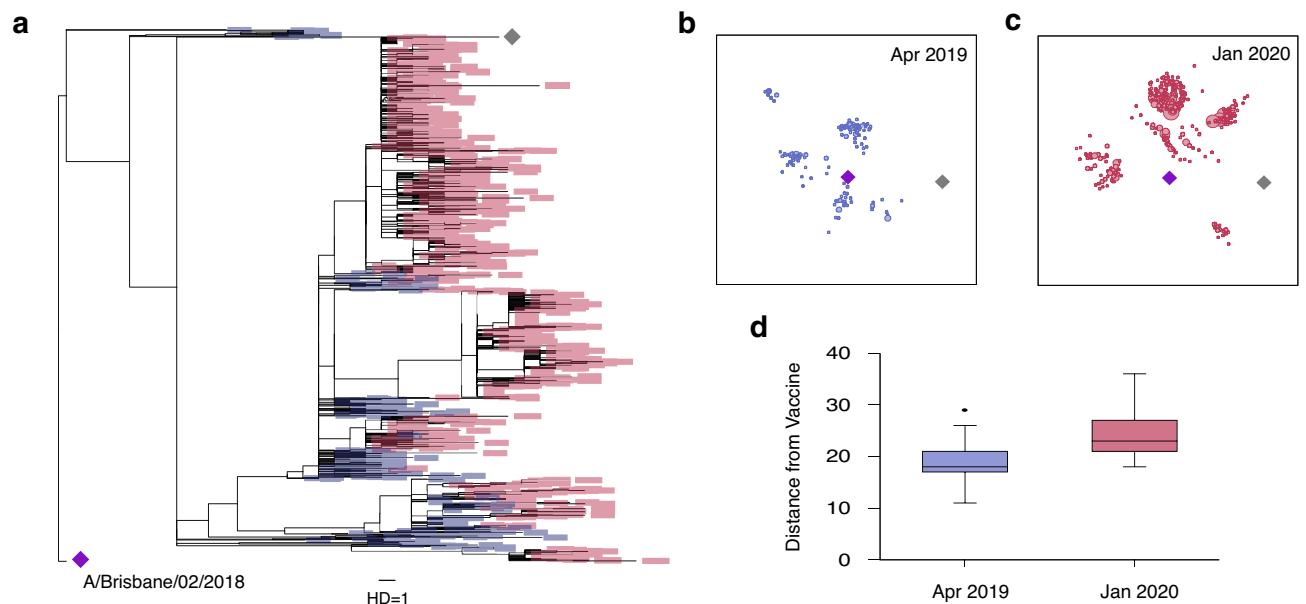


**Figure 4.** Influenza A (H1N1) evolution and vaccination. (a) Maximum likelihood tree of 255 H1N1 Hemagglutinin (HA) sequences sampled in April 2019 (blue boxes), 1140 H1N1 HA sequences sampled in January 2020 (red boxes), 2019–2020 H1N1 Northern hemisphere vaccine strain (A/Brisbane/02/2018, purple diamond) and 2018–2019 vaccine strain (A/Michigan/45/201, grey diamond). All HA nucleotide sequences were downloaded from GISAID<sup>20,21</sup>. The H1N1 HA sequences in January 2020 showed greater tree distances from the 2019–2020 H1N1 vaccine strain, compared to those in April 2019 (b) Two-dimensional map of 255 sequences collected in April 2019 along with the 2019–2020 H1N1 vaccine strain's HA sequence (purple diamond) and 2018–2020 H1N1 vaccine's HA sequence (grey diamond). The nucleotide distance among all pairs of sequences was scaled to the Euclidean distance by multidimensional scaling. (c) Two-dimensional map of 1140 HA sequences collected in January 2020 along with the two vaccine sequences. (d) The HA sequences in January 2020 showed greater nucleotide distances from the 2019–2020 vaccine strain than those in April 2019 ( $p < 0.001$ , Wilcoxon rank sum test).

This observed evolution away from the vaccine strain may explain the 2019–2020 seasonal influenza vaccine's low effectiveness against influenza A (H1N1). Influenza vaccine efficacy was estimated to be 37% against H1N1 strains during the 2019–20 flu season<sup>43</sup>. Viral evolution in response to vaccination remains a challenge for vaccine design, and the 2019–20 flu season highlights the need for real-time surveillance of viral sequences. Like influenza, SARS-CoV-2 has the potential to evolve in response to vaccination<sup>44</sup>, and thus SARS-CoV-2 evolution must be continuously monitored in real time to prevent vaccine failure and guide future vaccine strain selection.

## Discussion

We developed CorvGenSurv (Coronavirus Genomic Surveillance), a streamlined, high-resolution, and cost-effective SARS-CoV-2 whole genome sequencing method in which viral RNA is directly amplified, indexed, and sequenced. CorvGenSurv's precision and accuracy have been validated by Sanger sequencing and control genomic RNA sequencing, respectively. Our targeted amplification of the whole genome in three segments minimized the risk of genome coverage dropouts. Additionally, our streamlined long-read sequencing protocol significantly reduced workflow complexity and thus has a potential cost advantage over currently available short-read sequencing approaches<sup>8,10–12,26–28,31</sup>.

We obtained 25 whole genome sequences from NP/OP remnant COVID-19 positive test specimens that were collected from April to June 2020 at Los Angeles County, California, USA. The Los Angeles County pandemic accounted for 33% of all COVID-19 cases in California with around 3500 new cases per day in July 2020<sup>45,46</sup>. Our maximum likelihood tree analysis showed that the 25 strains were highly diverse within the G, GR and GH clades<sup>35</sup>. The G clade and its lineage have been dominant since late March, 2020 and its D614G mutation in the spike protein has been associated with increased transmissibility<sup>14</sup>. In addition to the G clade's other common mutation, NSP12-P323L, frequent mutations we observed include N-S194L, N-R203K, N-G204R, NSP2-T85I, and ORF3a-Q57H. From this wide spectrum of viral mutations, we estimated SARS-CoV-2 evolutionary rate by a Bayesian phylogenetic reconstruction method<sup>37,38</sup> and divergence measures. These two estimates were  $7.51 \times 10^{-4}$  and  $8.62 \times 10^{-4}$  substitutions per site per year respectively, which were consistent with recent reports on the SARS-CoV-2 evolutionary rate<sup>47–49</sup>.

We identified new amino acid mutations in the NSP3, NSP4, RdRP (NSP12), ORF8, and N proteins. Mutations in these proteins have the potential to trigger immune escape, alter viral replication capacity, or modulate viral immune suppression. Numerous T cell epitopes have been annotated in these proteins and thus mutations can lead to viral escape from cellular immune responses<sup>50,51</sup>. While mutations in the N, NSP3, NSP4 or NSP12 proteins can alter viral replication capacity<sup>13,52–55</sup>, those in the ORF8 or N proteins may dysregulate host innate

immune responses via type I interferon signal modulation<sup>54</sup>. It is therefore of great importance to monitor mutations from a diverse array of proteins by whole genome sequencing to pinpoint those that are relevant to viral pathogenicity and immune escape.

SARS-CoV-2's S protein is the key target for many of the vaccines currently in development<sup>18</sup> and thus mutations in this region are being closely monitored for their potential to render these vaccines ineffective. The observed influenza HA sequence evolution away from this year's vaccine strain clearly indicates the necessity of screening mutations in viral surface proteins. Genomic surveillance data can also inform SARS-CoV-2 drug resistance. Mutations in RdRP (NSP12) can potentially result in decreased binding affinity with nucleoside analogs such as Remdesivir and Favipiravir<sup>56</sup>. Therefore, genomic surveillance on circulating pandemic strains is crucial for guiding strategies for COVID-19 vaccination and therapeutic intervention and our simple and cost-efficient pipeline has the potential to advance real-time COVID-19 surveillance.

CorvGenSurv can accurately survey new mutations in real-time and thus provide crucial data for disease transmission, new outbreak detection, and vaccine candidate selection. As an alternative to the more common short-read sequencing approaches<sup>8,10–12,26–30</sup>, CorvGenSurv can facilitate the widespread adoption of real-time COVID-19 genomic surveillance and can therefore serve as an important tool for public health decision-making.

## Methods

**COVID-19 specimens at Keck School of Medicine Hospital of USC.** We accessed 25 de-identified nasopharyngeal (NP) and oropharyngeal (OP) remnant specimens which tested positive for COVID-19 via the Roche cobas<sup>®</sup> SARS-CoV-2 qualitative EUA assay at USC Clinical Laboratories, Keck Medicine of USC. These specimens were collected from Los Angeles County, California, USA between April 13th and June 22nd, 2020 (Table 1). This study (HS-20-00326) was approved by the Institutional Review Board of the University of Southern California as non-human subjects research. Table 1 lists each specimen's collection date and cycle threshold ( $C_t$ ) values for the ORF1 a/b non-structural SARS-CoV-2 unique region ( $C_{t-1}$ ) and the pan-Sarbecovirus conserved region in the structural protein envelope E-gene ( $C_{t-2}$ ).

**SARS-CoV-2 global strains.** We downloaded near full-length SARS-CoV-2 sequences from GISAID that were registered by July 27th, 2020. The sequences were globally aligned using MUSCLE<sup>57</sup>, and their 5'- and 3'-ends trimmed-out, yielding a 597–29340 segment of the Wuhan-Hu-1 reference strain. We removed any sequences that were shorter than this region and sequences with one or more ambiguous bases to obtain a total of 28,176 near full-length SARS-CoV-2 sequences, including 9339 originating from the USA and 1215 from California. In Table 1, all amino acid mutations from the reference sequence were annotated and novel mutations in our 25 sequences were reported.

**SARS-CoV-2 whole genome sequencing.** SARS-CoV-2 RNA was extracted from remnant NP/OP swab specimens in universal transport media using a MagMAX<sup>™</sup> Viral/Pathogen Nucleic Acid Isolation Kit with a KingFisher Duo Prime automated nucleic acid purification system (Thermo Fisher Scientific). A total of 20  $\mu$ l ( $15 \leq C_t < 20$ ), 100  $\mu$ l ( $20 \leq C_t < 25$ ), or 200  $\mu$ l ( $C_t \geq 25$ ) of viral media was diluted in 1 $\times$  PBS buffer to a total volume of 400  $\mu$ l and added to a deep-well plate for extraction using the manufacturer's protocol. Around 80  $\mu$ l of extracted SARS-CoV-2 RNA was recovered. This RNA was used as input for three separate 10 kb long RT-PCRs using the SuperScript<sup>™</sup> IV One-Step RT-PCR System (Thermo Fisher Scientific). As listed in Supplementary Table S1, the RT-PCR primers were 1\_LEFT/33\_RIGHT or For-c/Rev-c for the first segment, For-d/67\_RIGHT or 33\_LEFT/67\_RIGHT for the second segment, and 67\_LEFT/Rev-e or 67\_LEFT/98\_RIGHT for the third segment. Here, 1\_LEFT, 33\_RIGHT, 33\_LEFT, 67\_RIGHT, 67\_LEFT, and 98\_RIGHT were the ARTIC network primers (V3, <https://artic.network/ncov-2019>), where the "nCoV-2019\_" suffix was removed for simplicity. Primers, For-c, Rev-c, For-d, and Rev-e were designed in-house. These primers span the near full-length SARS-CoV-2 genome in three segments with overlap for genome assembly. The master mix was composed of 25  $\mu$ l RT-PCR master mix, 2.5  $\mu$ l each of 10  $\mu$ M forward and reverse primers, 0.5  $\mu$ l SuperScript IV RT mix, and 19.5  $\mu$ l of viral RNA to a total volume of 50  $\mu$ l. The samples were cycled according to the manufacturer's instructions: 50  $^{\circ}$ C for 10 min of RT, followed by 98  $^{\circ}$ C for 2 min for RT inactivation, then 35 cycles of 98  $^{\circ}$ C for 10 s, 55  $^{\circ}$ C for 10 s, 72  $^{\circ}$ C for 5 min, then a final extension of 72  $^{\circ}$ C for 5 min, held at 4  $^{\circ}$ C until the next step.

The RT-PCR products were then purified and concentrated with Ampure XP beads (Beckman Coulter) with a 0.8 $\times$  bead volume, two 70% ethanol washes, and elution in 25  $\mu$ l Nuclease-Free H<sub>2</sub>O. These purified RT-PCR products were subjected to long-range index PCR using PrimeSTAR GXL DNA Polymerase (Takara Bio) according to the manufacturer's instructions. After index PCR, product bands were confirmed via 1% agarose gel electrophoresis with the E-Gel Electrophoresis System (ThermoFisher, CA). Samples were equimolar pooled and shipped to DNA Technologies and Expression Analysis Core at UC Davis Genome Center for long-read, single-molecule, real-time (SMRT) sequencing on the PacBio Sequel II system with a 30-h movie.

**SARS-CoV-2 sanger sequencing.** Specimen, USA/CA-LAC-USC1, was selected for near full-length SARS-CoV-2 sequence confirmation via Sanger sequencing. Purified RT-PCR product for each of the three segments of USA/CA-LAC-USC1 was amplified via long-range PCR with the master mix composed of 10  $\mu$ l of PrimeSTAR GXL buffer, 4  $\mu$ l of dNTPs, 2.5  $\mu$ l each of 2  $\mu$ M forward and reverse primers, 1  $\mu$ l of PrimeSTAR GXL DNA polymerase, 26  $\mu$ l nuclease free H<sub>2</sub>O, and 4.0  $\mu$ l of purified RT-PCR product to a total volume of 50  $\mu$ l. The samples PCR cycled with 25 cycles of 98  $^{\circ}$ C for 10 s and 68  $^{\circ}$ C for 10 min, held at 4  $^{\circ}$ C until the next step. These products were Ampure cleaned with a 0.8 $\times$  bead volume and diluted to 20 ng/ $\mu$ l. A total of 10  $\mu$ l of the diluted product was combined with 5  $\mu$ l of each Sanger sequencing primer in 5  $\mu$ M. As listed in Supplementary Table S2, a total of 49 primers were selected from the V3 ARTIC network primers (<https://artic.network/>

ncov-2019) with minor modifications to minimize self-dimer and hairpin formation. The samples were then shipped to GENEWIZ (South Plainfield, NJ) for Sanger sequencing. The obtained sequences were subject to contig assembly using the CAP3 Sequence Assembly<sup>58</sup> followed by manual inspection, yielding USA/CA-LAC-USC1's near full-length SARS-CoV-2 genome (55–29,836).

**Consensus sequence building.** Each SARS-CoV-2 genome segment was de-multiplexed based on their indexes, creating one fasta file for each of the three segments per specimen. 100 reads were randomly picked from each fasta file and aligned using MUSCLE<sup>57</sup> to obtain a consensus sequence for each segment. The three segment consensus sequences were then assembled to produce each specimen's near full-length SARS-CoV-2 whole genome sequence (405–29,431).

**Maximum likelihood tree analysis and Bayesian phylogenetic analysis.** We used the PHYML program to produce maximum likelihood trees<sup>59</sup>. The general time-reversible model was used with the 'ML' option, and invariable sites were estimated with 12 substitution rate categories. The tree was generated by the BIONJ option. We used FigTree to present the obtained tree file.

BEAST42 v.1.10.4. was used to estimate the rate of SARS-CoV-2 evolution and divergence time<sup>37</sup>. The 25 SARS-CoV-2 near full-length genome sequences obtained in this study were input to BEAST along with its sample collection time (Table 1). Uncorrelated relaxed clock model with log-normal distribution was assumed with flexible skygrid coalescent tree priors and a single GTR +  $\Gamma$  substitution model<sup>38</sup>. The Monte Carlo (MCMC) length of chain was  $2 \times 10^6$ . The median evolution rate and divergence time along with respective 95% highest posterior density (HPD) were reported.

**Multi-dimensional scaling.** We globally aligned 5772 complete HA genome sequences that were collected between April 2019 and March 2020 along with two H1N1 vaccine strains A/Michigan/45/2015 and A/Brisbane/02/2018. These sequences were downloaded from GISAD<sup>20,21</sup>. The pairwise nucleotide base differences, Hamming Distance (HD), was measured and this HD matrix was input to a multi-dimensional scaling (MDS) algorithm from the python scikit-learn package (0.19.1). This MDS algorithm converted the HD matrix into a two-dimensional representation of the HA sequences by minimizing stress, the sum of squared distance of the disparities. Each sequence's position was updated until the stress difference was less than 0.1, and by repeating this procedure 400 times, the configuration with the minimum stress value was selected.

## Data availability

SARS-CoV-2 whole genome sequences sequenced in this study are available in GISAID (accession numbers EPI\_ISL\_569664-EIP\_ISL\_569688).

Received: 3 November 2020; Accepted: 21 June 2021

Published online: 01 July 2021

## References

1. Armstrong, G. L. *et al.* Pathogen genomics in public health. *N. Engl. J. Med.* **381**, 2569–2580 (2019).
2. Khoury, M. J. *et al.* From public health genomics to precision public health: A 20-year journey. *Genet. Med.* **20**, 574–582 (2018).
3. Peters, P. J. *et al.* HIV infection linked to injection use of oxycodone in Indiana, 2014–2015. *N. Engl. J. Med.* **375**, 229–239 (2016).
4. Gardy, J. L. *et al.* Whole-genome sequencing and social-network analysis of a tuberculosis outbreak. *N. Engl. J. Med.* **364**, 730–739 (2011).
5. Quick, J. *et al.* Real-time, portable genome sequencing for Ebola surveillance. *Nature* **530**, 228–232 (2016).
6. Arias, A. *et al.* Rapid outbreak sequencing of Ebola virus in Sierra Leone identifies transmission chains linked to sporadic cases. *Virus Evol.* **2**, vew016 (2016).
7. Giovanetti, M. *et al.* Genomic and Epidemiological Surveillance of Zika Virus in the Amazon Region. *Cell Rep* **30**, 2275–2283 (2020).
8. Gudbjartsson, D. F. *et al.* Spread of SARS-CoV-2 in the Icelandic population. *N. Engl. J. Med.* **382**, 2302–2315 (2020).
9. Pung, R. *et al.* Investigation of three clusters of COVID-19 in Singapore: Implications for surveillance and response measures. *Lancet* **395**, 1039–1046 (2020).
10. Oude Munnink, B. B. *et al.* Rapid SARS-CoV-2 whole-genome sequencing and analysis for informed public health decision-making in the Netherlands. *Nat. Med.* **26**, 1405–1410 (2020).
11. Rockett, R. J. *et al.* Revealing COVID-19 transmission in Australia by SARS-CoV-2 genome sequencing and agent-based modeling. *Nat. Med.* **26**, 1398–1404 (2020).
12. Wu, F. *et al.* A new coronavirus associated with human respiratory disease in China. *Nature* **579**, 265–269 (2020).
13. Gao, Y. *et al.* Structure of the RNA-dependent RNA polymerase from COVID-19 virus. *Science* **368**, 779–782 (2020).
14. Korber, B. *et al.* Tracking changes in SARS-CoV-2 spike: Evidence that D614G increases infectivity of the COVID-19 virus. *Cell* **182**, 812–827 (2020).
15. Davies, N. G. *et al.* Increased mortality in community-tested cases of SARS-CoV-2 lineage B.1.1.7. *Nature*. **593**, 270–274 (2021).
16. Garcia-Beltran, W. F. *et al.* Multiple SARS-CoV-2 variants escape neutralization by vaccine-induced humoral immunity. *Cell* <https://doi.org/10.1016/j.cell.2021.03.013> (2021).
17. Zhou, D. *et al.* Evidence of escape of SARS-CoV-2 variant B.1.351 from natural and vaccine-induced sera. *Cell*. **184**, 2348–2361 (2021).
18. Callaway, E. The race for coronavirus vaccines: A graphical guide. *Nature* **580**, 576–577 (2020).
19. Folegatti, P. M. *et al.* Safety and immunogenicity of the ChAdOx1 nCoV-19 vaccine against SARS-CoV-2: A preliminary report of a phase 1/2, single-blind, randomised controlled trial. *Lancet* **396**, 467–478 (2020).
20. Elbe, S. & Buckland-Merrett, G. Data, disease and diplomacy: GISAID's innovative contribution to global health. *Glob Chall* **1**, 33–46 (2017).
21. Shu, Y. & McCauley, J. GISAID: Global initiative on sharing all influenza data—From vision to reality. *Euro Surveill.* **22**, 30494 (2017).

22. Hadfield, J. *et al.* Nextstrain: Real-time tracking of pathogen evolution. *Bioinformatics* **34**, 4121–4123 (2018).
23. Belongia, E. A. *et al.* Variable influenza vaccine effectiveness by subtype: A systematic review and meta-analysis of test-negative design studies. *Lancet Infect. Dis.* **16**, 942–951 (2016).
24. Zost, S. J. *et al.* Contemporary H3N2 influenza viruses have a glycosylation site that alters binding of antibodies elicited by egg-adapted vaccine strains. *Proc. Natl. Acad. Sci. U S A* **114**, 12578–12583 (2017).
25. Yin, W. *et al.* Structural basis for inhibition of the RNA-dependent RNA polymerase from SARS-CoV-2 by remdesivir. *Science* **368**, 1499–1504 (2020).
26. Xiao, M. *et al.* Multiple approaches for massively parallel sequencing of SARS-CoV-2 genomes directly from clinical samples. *Genome Med.* **12**, 57 (2020).
27. Gonzalez-Reiche, A. S. *et al.* Introductions and early spread of SARS-CoV-2 in the New York City area. *Science* **369**, 297–301 (2020).
28. Meredith, L. W. *et al.* Rapid implementation of SARS-CoV-2 sequencing to investigate cases of health-care associated COVID-19: A prospective genomic surveillance study. *Lancet Infect. Dis.* **20**, 1236–1271 (2020).
29. Paden, C. R. *et al.* Rapid, sensitive, full-genome sequencing of severe acute respiratory syndrome coronavirus 2. *Emerg. Infect. Dis.* **26**, 2401–2405 (2020).
30. Li, T. *et al.* Rapid high throughput whole genome sequencing of SARS-CoV-2 by using one-step RT-PCR amplification with integrated microfluidic system and next-gen sequencing. *J. Clin. Microbiol.* <https://doi.org/10.1128/JCM.02784-20> (2021).
31. Quick, J. *et al.* Multiplex PCR method for MinION and Illumina sequencing of Zika and other virus genomes directly from clinical samples. *Nat. Protoc.* **12**, 1261–1276 (2017).
32. Eid, J. *et al.* Real-time DNA sequencing from single polymerase molecules. *Science* **323**, 133–138 (2009).
33. Wenger, A. M. *et al.* Accurate circular consensus long-read sequencing improves variant detection and assembly of a human genome. *Nat. Biotechnol.* **37**, 1155–1162 (2019).
34. Sanger, F., Nicklen, S. & Coulson, A. R. DNA sequencing with chain-terminating inhibitors. *Proc. Natl. Acad. Sci. USA* **74**, 5463–5467 (1977).
35. Mercatelli, D. & Giorgi, F. M. Geographic and genomic distribution of SARS-CoV-2 mutations. *Front. Microbiol.* **11**, 1800 (2020).
36. Deng, X. *et al.* Genomic surveillance reveals multiple introductions of SARS-CoV-2 into Northern California. *Science* **369**, 582–587 (2020).
37. Suchard, M. A. *et al.* Bayesian phylogenetic and phylodynamic data integration using BEAST 1.10. *Virus Evol.* **4**, vey016 (2018).
38. Boni, M. F. *et al.* Evolutionary origins of the SARS-CoV-2 sarbecovirus lineage responsible for the COVID-19 pandemic. *Nat. Microbiol.* **5**, 1408–1417 (2020).
39. Long, S. W. *et al.* Sequence analysis of 20,453 severe acute respiratory syndrome coronavirus 2 genomes from the Houston metropolitan area identifies the emergence and widespread distribution of multiple isolates of all major variants of concern. *Am. J. Pathol.* <https://doi.org/10.1016/j.ajpath.2021.03.004> (2021).
40. Kennedy, D. A. & Read, A. F. Monitor for COVID-19 vaccine resistance evolution during clinical trials. *PLoS Biol.* **18**, e3001000 (2020).
41. Petrova, V. N. & Russell, C. A. The evolution of seasonal influenza viruses. *Nat. Rev. Microbiol.* **16**, 60 (2018).
42. [https://www.who.int/influenza/vaccines/virus/recommendations/201902\\_recommendation.pdf](https://www.who.int/influenza/vaccines/virus/recommendations/201902_recommendation.pdf). Accessed 24 June 2021.
43. [https://www.cdc.gov/mmwr/volumes/69/wr/mm6907a1.htm?s\\_cid=mm6907a1\\_w](https://www.cdc.gov/mmwr/volumes/69/wr/mm6907a1.htm?s_cid=mm6907a1_w). Accessed 24 June 2021.
44. De Groot, A. S. How the SARS vaccine effort can learn from HIV-speeding towards the future, learning from the past. *Vaccine* **21**, 4095–4104 (2003).
45. <https://www.latimes.com/projects/california-coronavirus-cases-tracking-outbreak/>. Accessed 24 June 2021.
46. [http://dashboard.publichealth.lacounty.gov/covid19\\_surveillance\\_dashboard/](http://dashboard.publichealth.lacounty.gov/covid19_surveillance_dashboard/). Accessed 24 June 2021.
47. MacLean, O. A., Orton, R. J., Singer, J. B. & Robertson, D. L. No evidence for distinct types in the evolution of SARS-CoV-2. *Virus Evol.* **6**, veaa034 (2020).
48. <https://virological.org/t/phylodynamic-analysis-176-genomes-6-mar-2020/356>. Accessed 24 June 2021.
49. Su Y. C. *et al.* Discovery of a 382-nt deletion during the early evolution of SARS-CoV-2. *bioRxiv*. <https://doi.org/10.1101/2020.03.11.987222> (2020).
50. Grifoni, A. *et al.* Targets of T cell responses to SARS-CoV-2 coronavirus in humans with COVID-19 disease and unexposed individuals. *Cell* **181**, 1489–1501 (2020).
51. Grifoni, A. *et al.* A Sequence homology and bioinformatic approach can predict candidate targets for immune responses to SARS-CoV-2. *Cell Host Microbe* **27**, 671–680 (2020).
52. McBride, R., van Zyl, M. & Fielding, B. C. The coronavirus nucleocapsid is a multifunctional protein. *Viruses* **6**, 2991–3018 (2014).
53. Lei, J., Kusov, Y. & Hilgenfeld, R. Nsp3 of coronaviruses: Structures and functions of a large multi-domain protein. *Antiviral Res.* **149**, 58–74 (2018).
54. Li, J. Y. *et al.* The ORF6, ORF8 and nucleocapsid proteins of SARS-CoV-2 inhibit type I interferon signaling pathway. *Virus Res.* **286**, 198074 (2020).
55. Sakai, Y. *et al.* Two-amino acids change in the nsp4 of SARS coronavirus abolishes viral replication. *Virology* **510**, 165–174 (2017).
56. Agostini, M. L. *et al.* Coronavirus susceptibility to the antiviral Remdesivir (GS5734) is mediated by the viral polymerase and the proofreading exoribonuclease. *mBio* **9**, e00221–e00218 (2020).
57. Edgar, R. C. MUSCLE: Multiple sequence alignment with high accuracy and high throughput. *Nucleic Acids Res.* **32**, 1792–1797 (2004).
58. Huang, X. & Madan, A. CAP3: A DNA sequence assembly program. *Genome Res.* **9**, 868–877 (1999).
59. Guindon, S. & Gascuel, O. A simple, fast, and accurate algorithm to estimate large phylogenies by maximum likelihood. *Syst. Biol.* **52**, 696–704 (2003).

## Acknowledgements

We thank the Molecular Pathology Division of the USC Keck Clinical Laboratories for providing the remnant NP/OP specimens that are sequenced in this study. The genomic RNA of USA-WA1/2020 strain was deposited by the Centers for Disease Control and Prevention and obtained through BEI Resources, NIAID, NIH: Genomic RNA from SARS-Related Coronavirus 2, Isolate USA-WA1/2020, NR-52285. We thank Dr. Jing-Hsiung James Ou, Dr. Sarah Hamm-Alvarez, and Dr. Thomas Buchanan for their help. We thank all laboratories and authors who shared global SARS-CoV-2 whole genome sequences and influenza H1N1 Hemagglutinin (HA) sequences by depositing to GISAID's EpiFlu (TM) Database.

## Author contributions

H.L. and S.P. conceived this project, designed the experimental workflows and bioinformatics pipelines, and performed sequence analysis. G.F. conducted SARS-CoV-2 whole genome sequencing. P.W. and J.E. provided COVID-19 remnant specimens sequenced in this study.

### Competing interests

The authors declare no competing interests.

### Additional information

**Supplementary Information** The online version contains supplementary material available at <https://doi.org/10.1038/s41598-021-93145-4>.

**Correspondence** and requests for materials should be addressed to H.Y.L.

**Reprints and permissions information** is available at [www.nature.com/reprints](http://www.nature.com/reprints).

**Publisher's note** Springer Nature remains neutral with regard to jurisdictional claims in published maps and institutional affiliations.



**Open Access** This article is licensed under a Creative Commons Attribution 4.0 International License, which permits use, sharing, adaptation, distribution and reproduction in any medium or format, as long as you give appropriate credit to the original author(s) and the source, provide a link to the Creative Commons licence, and indicate if changes were made. The images or other third party material in this article are included in the article's Creative Commons licence, unless indicated otherwise in a credit line to the material. If material is not included in the article's Creative Commons licence and your intended use is not permitted by statutory regulation or exceeds the permitted use, you will need to obtain permission directly from the copyright holder. To view a copy of this licence, visit <http://creativecommons.org/licenses/by/4.0/>.

© The Author(s) 2021